http://dx.doi.org/10.5012/bkcs.2011.32.10.3575

Controlled Assembly of Gold Nanoprism and Hexagonal Nanoplate Films for Surface Enhanced Raman Scattering

Doori Lee,[†] Soonchang Hong,[†] and Sungho Park[†,‡,§,*]

[†]*Department of Chemistry,* [‡]*Department of Energy Science,* [§]*SKKU Advanced Institute of Nanotechnology, Sungkyunkwan University, Suwon 440-746, Korea.* [*]*E-mail: Spark72@skku.edu*
Received July 8, 2011, Accepted August 5, 2011

This paper reports a methodology for preparing close-packed two dimensional gold nanoprism films and hexagonal nanoplate films at a hexane/water interface. By controlling the concentration of linker molecules in the hexane layer and the temperature of the colloid solution, highly ordered close-packed nanoplate arrays can be fabricated. These films were investigated to compare their corresponding surface enhanced Raman scattering (SERS) efficiencies. It was demonstrated that the Au nanoprism films resulted in a stronger SERS enhancement than the Au hexagonal nanoplate films. The difference in the SERS enhancement is attributed to the film array difference, demonstrating that Au nanoprism films have a higher line contact density than their Au hexagonal analogues.

Key Words : Gold nanoprism, Gold hexagonal nanoplate, Gold film, Surface enhanced Raman scattering

Introduction

Two or three dimensional assemblies of nanoparticles have been fabricated through various methods including solvent evaporation,[1,2] covalent attachment,[3,4] layer-by-layer sequential adsorption technique,[5,6] and the Langmuir Blodgett method.[7-9] These assemblies show distinctly different properties compared to nanoparticles prepared *via* colloidal solutions. For example, the extinction spectra of metal nanoparticle films are broader and more red shifted than the spectra of colloidal solutions due to the strong electronic coupling between nanoparticles.[10] However, assemblies of nanoparticles have been limited to isotropic nanoparticles because most research in the past several decades has focused on synthesis or application of isotropic spherical nanoparticles.[11-13] Recently, as synthetic routes for anisotropic nanoparticles have become well developed,[14-16] their potential importance in applications has been drawing great interest. In particular, plate-shaped nanoparticles such as nanoprism, nanodisks, and hexagonal nanoplates have great potential applications in optical devices,[17] electronic devices,[18,19] and active substrates for SERS.[20] From this point of view, it is worth fabricating two-dimensional assemblies of plate-shaped nanoparticles.

In our previous work, we fabricated two or three dimensional arrays with Au spherical nanoparticles and nanorods at a hexane/water interface by utilizing the interfacial energy stabilization between the organic and water media.[21] Linker molecules in a hexane layer were a key factor to fabricate highly ordered close-packed nanoparticles arrays. Although it is possible to trap nanoplates at the water/hexane interface through the identical concept, nanoplates were not homogenously ordered under similar experimental conditions. This study investigated how to efficiently form close-packed two-dimensional nanoplate films by decreasing the trapping rate of nanoplates through temperature control of the colloid solution. In addition, the corresponding optical properties including SERS enhancement were characterized.

Experimental Section

Au nanoprisms were prepared according to the method reported in the literature.[15,22] Briefly, citrate-stabilized small gold nanoparticle seeds (d = 4-6 nm) were prepared by $NaBH_4$ reduction of $HAuCl_4$. 1 mL of the seed solution was added to the growth solution (labeled as 1) containing a surfactant (cetyl-trimethylammonium bromide), Au ions (hydrogen tetrachloroaurate), a reducing agent (L-ascorbic acid), iodide ions (sodium iodide) and NaOH. 1 mL of the growth solution 1 was added to the growth solution 2, which was identical to the growth solution 1. All of the growth solution 2 was added to the growth solution 3, which contained identical reagents but at 10 times as much as the growth solutions 1 and 2. The average edge length and thickness were determined by field emission scanning electron microscopy (FESEM) to be 160 ± 14 nm and 8 ± 1 nm, respectively. Field emission scanning electron microscopy images were obtained using a JEOL 7000F and a JEOL 7600F.

Au hexagonal nanoplates were prepared by using nanoprisms as seeds according to the literature method.[23] Briefly, 3 mL of nanoprism solution was added to a solution containing a surfactant (CTAB), small amounts of iodide ions (sodium iodide), and Au ions (hydrogen tetrachloroaurate). Then, a reducing agent (L-ascorbic acid) was added dropwise. The average edge length and thickness were determined by field emission scanning electron microscopy (FESEM) to be 256 ± 27 nm and 19 ± 2 nm, respectively.

Figure 1 shows a schematic diagram of the fabrication of the 2-dimensional assemblies with Au nanoprisms and

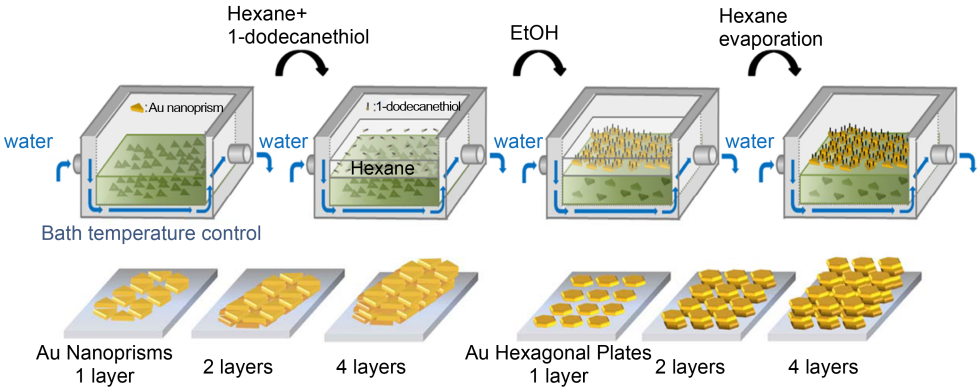

Figure 1. Schematic presentation of the gold nanoplate film formation process at the hexane/water interface.

hexagonal nanoplates at the water/hexane interface. 30 mL of the nanoplate aqueous solution was transferred to a Teflon cell (inner dimension, 7.5 × 4.0 × 2.0 cm) surrounded by water which was connected to a circulator to control the temperature of the colloid solution. 10 mL of hexane was added to the top of the colloid solution to form an immiscible hexane/water interface and a controlled amount of 1-dedocanethiol was added to the hexane layer. Then, about 9 mL of ethanol was added dropwise at a rate of 0.5 mL/min using a mechanical syringe pump, KDS101, supplied by Kd Scientific Inc., to extract nanoplates from the aqueous solution to the hexane/water interface. The detailed process to fabricate the 2-dimensional array of nanoplate films can be found in a previous publication.[21] The desired nanoplate films were transferred onto glass and silicon wafer for UV-vis absorption spectra, FESEM, and SERS measurements.

A micro-Raman spectrometer (Renishaw, InVia) was used to record the SERS. A He-Ne laser at 632.8 nm was used as the excitation laser. The excitation light of less than 0.5 mW was focused onto a sample area of approximately 1 μm^2. Each Raman spectrum was obtained with a 10 s exposure time to the detector. 0.1 M of mercaptobenzene in ethanol was used as the analyte for the SERS measurement

Results and Discussions

We previously reported a methodology for fabricating highly ordered spherical metal nanoparticle films through in-situ coating of nanoparticles with 1-dodecanethiol.[21] These long-chain alkanethiols convert the electrostatic repulsion of metal nanoparticles into van der Waals interactions. Here, the identical concept was applied to Au nanoprisms and hexagonal nanoplates. Figure 2 shows representative FESEM and UV-vis absorption spectra of Au nanoprism films as functions of the amount of 1-dodecanethiols in the hexane layer and the temperature of the colloid solutions. Irreversible coagulation of nanoprisms at the interface was observed when no 1-dodecanethiol was added at room temperature (RT) (Figure 2B-1). As ethanol was added to the aqueous colloid solution, nanoparticles were entrapped at the hexane/water interface because the surface charge density of the nanoparticles decreased, leading to reduction of the interfacial energy at the hexane/water interface.[24] However, nanoparticles at the interface became less stable than dispersed one in the solution due to the reduced electrostatic repulsion force. Additionally, the surface charges of nanoparticles are distributed asymmetrically at the interface, which leads to a strong capillary attraction.[25,26] These destabilized nanoparticles became more stable through the irreversible aggregation process. It is known that irreversible coagulation occurs when the induced capillary attraction is stronger than the nanoparticles electrostatic repulsive force.[25,26]

Figure 2B-2 shows that some of the nanoprisms were etched like nanodisks and other nanoprisms were fused irreversibly when 4.17×10^{-5} M 1-dodecanethiol was present in the hexane layer at room temperature. Approximately, a total number of 1.21×10^5 molecules are required to fully coat the surface of a single nanoprism, by assuming the edge length of nanoprism is 160 nm and the van der Waals dimensions of the thiol head group[27] is 21.4 $Å^2$. The used volume of 3 mL of 4.17×10^{-5} M 1-dodecanethiol is equivalent to a total number of $\sim 7.53 \times 10^{16}$ molecules. Therefore, there were sufficient 1-dodecanethiols in hexane to fully coat entrapped nanoprisms at the interface. However, all of the existing 1-dodecanethiols cannot be adsorbed to the surface of nanoprisms because the molecules were dispersed in a total volume of 13 mL of hexane. The observed shape-distortion indicates that the surface of nanoprisms was not fully passivated by 1-dodecanethiols. It is worthy to note that the vertex site atoms of a nanoprism have a lower coordination number (CN) than the terrace sites[28,29] and therefore the vertex site is more labile (i.e. unstable) than flat terrace site under etching environment. In addition, the basal planes of the nanoprism are the {111} plane and the side planes are the {112} plane,[22] which leads to a high surface energy at the vertex sites and side planes.[30] These indicates that the vertex sites and side planes of the nanoprism are labile and can cause shape transformation. As a result, some of the nanoprisms that are not fully covered with molecules will be transformed to nanodisks, and other nanoplates that are not covered with molecules will aggregate.

When the films were prepared using 4.17×10^{-4} M 1-dodecanethiol at RT, the nanoprisms preserved their charac-

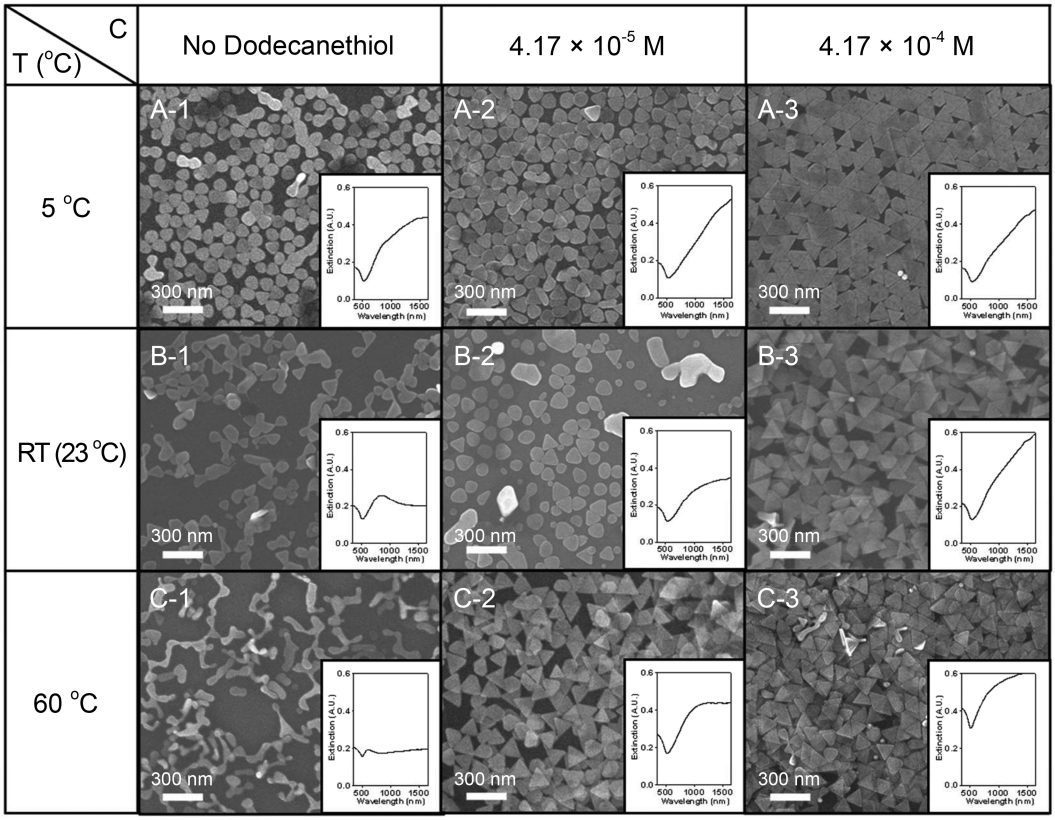

Figure 2. FESEM images and UV-vis absorption spectra of (bottom right insets) of the nanoprism films. The films were prepared in the presence of 1-dodecanethiol (A-1) 0 M, (A-2) 4.17×10^{-5} M, and (A-3) 4.17×10^{-4} M in the hexane layer at 5 °C. Nanoprism films without (B-1), with (B-2) 4.17×10^{-5} M, and (A-3) 4.17×10^{-4} M 1-dodecanethiol in the hexane layer at RT. Nanoprism films without (C-1), with (C-2) 4.17×10^{-5} M, and (C-3) 4.17×10^{-4} M 1-dodecanethiol in the hexane layer at 60 °C.

teristic sharp vertices, as shown in Figure 2B-3. In this case, sufficient molecules (2.78×10^6 molecules per a single nanoprism) can fully cover each nanoprism that was entrapped at the interface and these molecules prevented them from experiencing the shape transformation and coagulation. Even though nanoprism films were fabricated with a sufficient amount of 1-dodecanethiols, these films were not highly ordered. Some parts of the films exhibited multilayer and other parts showed large voids due to the strong attractive force between the alkanethiol-decorated nanoprism surfaces.[31] Furthermore, when nanoprisms were fully coated with hydrophobic 1-dodecanethiols, the nanoprisms would be attracted to hexane layer, leaving from the interface. This will induce the formation of multilayer of nanoprisms because it opens additional space for the second nanoprism entrapment. The Coulombic repulsion forces of nanoprisms in water are not strong enough to prevent stacking of the nanoprisms. It is noteworthy that the stabilizing interfacial energy is proportional to the particle size (R^2) and temperature (T) as nanoparticles are entrapped at the interface.[32] The nanoprisms have a large cross sectional area compared to reported spherical nanoparticles (d = 13-90 nm). Hence, the magnitude of the stabilizing interfacial energy is much larger with flat nanoprisms than spherical nanoparticles. Rapid entrapment of nanoprism occurs due to the large stabilizing interfacial energy. In conclusion, the larger interfacial stabilization energy and the flat geometry of the nanoplate give rise to the formation of inhomogeneous multilayer arrays.

To fabricate homogeneously ordered nanoprism films, the temperature of the colloid solutions was controlled while keeping the other experimental conditions constant. Figure 2A-1, -2 and -3 show nanoprism films formed at 5 °C. When 4.17×10^{-4} M 1-dodecanethiol was present in the hexane layer at 5 °C close-packed 2-dimensional array (*ca*. 92.4%) was fabricated, as shown in Figure 2A-3 (See the supporting information, Figure S2 for larger domain image). The stabilizing interfacial energy of nanoprism entrapment at 5 °C is smaller and the trapping rate at 5 °C is slower than RT because the stabilizing energy depends on the temperature. [34] This reduced trapping rate allows enough time for the rearrangement of entrapped nanoprisms before another nanoprism is trapped and stacked. The highly ordered nanoprism arrays retained their characteristic shape and sharp vertices because sufficient amounts of 1-dodecanethiol blocked the fusion of nanoprisms. When 1-dodecanethiol was not added or 4.17×10^{-5} M 1-dodecanethiol was added in the hexane layer at 5 °C, the fabricated films showed 2-dimensional arrays but most of nanoprisms were etched or fused (Figure 2A-1 and 2A-2) because insufficient alkanethiols could not fully passivate the nanoprisms. At high temperature (60 °C) without 1-dodecanethiol, Figure 2C-1 shows

that the nanoprisms were severely fused. When 4.17×10^{-4} M 1-dodecanethiol was added in the hexane layer at 60 °C, the fabricated films had a similar morphology to the sample prepared at RT but with more multilayer stacking, as shown in Figure 2C-3, due to the rapid trapping rate at high temperature (*vide supra*). Even though the nanoprisms were randomly ordered, when insufficient molecules (4.17×10^{-5} M alkanethiols) were added at 60 °C, the nanoprisms retained their sharp vertices, which is distinctly different from the RT result (Figure 2C-2). The kinetic energy of Brownian motion is proportional to temperature ($E = 3KT/2$).[33-35] It is expected that 1-dodecanethiol in the hexane layer has a higher kinetic energy at 60 °C than RT. Therefore, molecules would have a greater chance to passivate entrapped nanoprisms at higher temperature.

The bottom right inset in each SEM image of Figure 2 shows the UV-vis absorption spectrum corresponding to each SEM image. Most of the spectra did not show any characteristic feature of nanoprism surface plasmon energy bands and showed a profile of metal films due to the strong electromagnetic coupling between nanoparticles (See Supporting Information, Figure S1 for the spectrum of nanoplates when dispersed in water freely). However, the absorption intensity increased depending on the stacking magnitude.

This method of controlling the concentration of alkanethiols and temperature of the colloid solution can be applied to other shapes of nanoplates synthesized in an aqueous medium. Figure 3 shows FESEM images and the corresponding UV-vis absorption spectra for each film fabricated with hexagonal nanoplates by following the same method used for the nanoprisms. Highly ordered hexagonal nanoplate films could not be fabricated regardless the concentration of 1-dodecanethiols at RT, as shown Figure 3B-1-3. Even though hexagonal nanoplates are more stable than nanoprisms at the interface due to their large size, the fusion of the nanoplate vertices was observed when no 1-dodecanethiol was added. When the temperature of hexagonal colloid solution decreased, closed-packed hexagonal nanoplate arrays (*ca.* 94.4%) were well fabricated with certain amounts of alkanethiols (Figure 3A-3) (See the supporting information, Figure S3 for larger domain image). At high temperature (60 °C), Figure 3C-1 displays that neighboring nanoplates were interwoven with each other when no 1-dodecanethiol was present. Even vertically aligned hexagonal nanoplates were observed at this temperature. A high temperature would supply sufficient kinetic energy and it led to vertically aligned nanoplates at the interface. The bottom right inset in each SEM image in Figure 3 shows UV-vis absorption spectrum corresponding to each SEM image. Due to strong electromagnetic coupling between nanoplates, no surface plasmon peak was observed except for fused nanoplate films.

Well-fabricated close-packed 2-dimensional nanoprisms

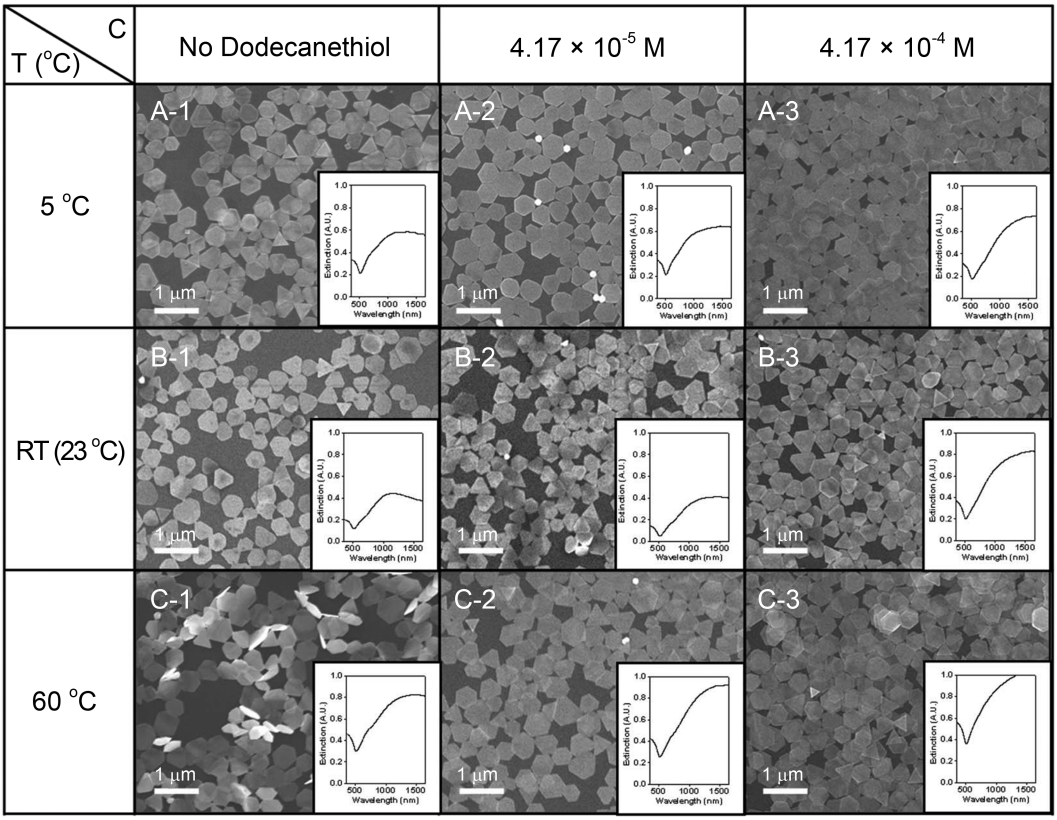

Figure 3. FESEM images and UV-vis absorption spectra (bottom right insets) of the hexagonal nanoplate films. The films were prepared in the presence of 1-dodecanethiol (A-1) 0 M, (A-2) 4.17×10^{-5} M, and (A-3) 4.17×10^{-4} M in the hexane layer at 5 °C. Hexagonal nanoplate films without (B-1), with (B-2) 4.17×10^{-5} M, and (A-3) 4.17×10^{-4} M 1-dodecanethiol in the hexane layer at RT. Hexagonal nanoplate films without (C-1), with (C-2) 4.17×10^{-5} M, and (C-3) 4.17×10^{-4} M 1-dodecanethiol in the hexane layer at 60 °C.

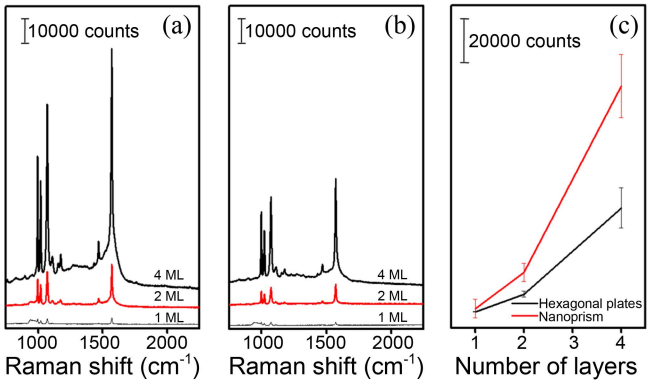

Figure 4. SERS spectra of adsorbed mercaptobenzene: (a) on Au nanoprism films; (b) on Au hexagonal nanoplate films. A graph for SERS intensity of a band at 1572 cm^{-1} *vs* different number of nanoprism film and hexagonal plate film monolayers.

and hexagonal nanoplate films were utilized as SERS substrates to compare their SERS enhancements as a function of the number of layers. Figure 4(a) shows the SERS spectrum of mercaptobenzene adsorbed on nanoprism and Figure 4(b) shows the SERS spectrum of hexagonal plate films. The assignment of peaks in the SERS spectra has been previously reported and will not be mentioned in this report[36-38] as the purpose of this report is to compare the relative SERS enhancement on nanoprism and hexagonal plate films. In previous works, we reported the nanorods films had a stronger SERS enhancement than nanosphere films because nanorods films had line contacts among the nanorods, which induces strong electromagnetic coupling, often referred to as "hot spot" coupling.[39-44] When nanoprisms are assembled, 3 lateral line contacts can be generated while hexagonal nanoplate can generate 6 line contacts. Therefore, hexagonal nanoplate films are expected to show stronger enhancement in the SERS spectra because of the larger contact density of hexagonal nanoplates in the same area if they are identically sized. However, the nanoprism films exhibited a 1.5 times stronger enhancement than the hexagonal nanoplate films because the edge length of the hexagonal plate was 1.6 times longer than that of the nanoprisms, as shown in Figure 4. Nanoprism films have 22.7 μm line contacts in a 1 μm^2 excitation beam area while hexagonal films have 4.9 μm line contacts in the same area. By assuming close packing, nanoprisms films have a 4.6 times larger line density (*line density = line contact length/excitation beam spot area*). Figure 4(c) shows the SERS intensity increase linearly as the number of layers increase.

Conclusion

This paper reports a method for preparing highly ordered gold nanoprism films and hexagonal nanoplate films. Controlling the temperature of the colloid solutions and concentration of 1-dodecanethiol is critical for fabricating close-packed 2-dimension nanoplate films. These highly ordered nanoplate films have potential applications in optics and electronics.

Acknowledgments. This work was supported by the National Research Foundation of Korea (World Class University (WCU): R31-2008-10029, Nano R&D program: 2010-0019149, 2010-0015457, and Priority Research Centers Program: NRF-20100029699).

References

1. Rabani, E.; Reichman, D. R.; Geissler, P. L.; Brus, L. E. *Nature* **2003**, *426*, 271.
2. Stannard, A.; Martin, C. P.; Pauliac-Vaujour, E.; Moriarty, P.; Thiele, U. *J. Phys. Chem. C* **2008**, *112*, 15195.
3. Bandyopadhyay, K., Patil, V.; Vijayamohanan, K.; Sastry, M. *Langmuir* **1997**, *13*, 5244.
4. Liu, X., Liu, H.; Zhou, W.; Zheng, H.; Yin, X.; Li, Y. *Langmuir* **2010**, *26*, 3179.
5. Crisp, M. T.; Kotov, N. A. *Nano Lett.* **2003**, *3*, 173.
6. Srivastava, S.; Kotov, N. A. *Acc. Chem. Res.* **2008**, *41*, 1831.
7. Collier, C. P.; Saykally, R. J.; Shiang, J. J.; Henrichs, S. E.; Heath, J. R. *Science* **1997**, *277*, 1978.
8. Lee, D. K.; Kang, Y. S., Lee, C. S.; Stroeve, P. *J. Phys. Chem. B* **2002**, *106*, 7267.
9. Gole, A.; Jana, N. R.; Selvan, S. T.; Ying, J. Y. *Langmuir* **2008**, *24*, 8181.
10. Yun, S.; Oh, M. K.; Kim, S. K.; Park, S. *J. Phys. Chem. C* **2009**, *113*, 13551.
11. Wilcoxon, J. P.; Provencio, P. P. *J. Am. Chem. Soc.* **2004**, *126*, 6402.
12. Kim, P. P.; Oh, S.; Crooks, R. M. *Chem. Mater.* **2004**, *16*, 167.
13. Pastoriza-Santos, I.; Liz-Marzan, L. M. *Langmuir* **2002**, *18*, 2888.
14. Gou, L.; Murphy, C. J. *Chem. Mater.* **2005**, *17*, 3668.
15. Millstone, J. E.; Park, S.; Shuford, K. L.; Qin, L.; Schatz, G. C.; Mirkin, C. A. *J. Am. Chem. Soc.* **2005**, *127*, 5312.
16. Okitsu, K.; Sharyo, K.; Nishimura, R. *Langmuir* **2009**, *25*, 7786.
17. Xue, C.; Li, Z.; Mirkin, C. A. *Small* **2005**, *1*, 513.
18. Wenjing, L.; Houyi, M.; Jintao, Z.; Xiuyu, L.; Xingli, F. *J. Phys. Chem. C* **2009**, *113*, 1738.
19. Goyal, R. N.; Aliumar, A.; Oyama, M. *J. Electroanal. Chem.* **2009**, *631*, 58.
20. Xiong, Y.; McLellan, J. M.; Chen, J.; Yin, Y.; Li, Z.-Y.; Xia, Y. *J. Am. Chem. Soc.* **2005**, *127*, 17118.
21. Park, Y.-K.; Yoo, S.-H.; Park, S. *Langmuir* **2007**, *23*, 10505.
22. Millstone, J. E.; Metraux, G. S.; Mirkin, C. A. *Adv. Funct. Mater.* **2006**, *16*, 1209.
23. Hong, S.; Shuford, K. L.; Park, S. *Chem. Mater.* **2011**, *23*, 2011.
24. Reincke, F.; Kegel, W. K.; Zhang, H.; Nolte, M.; Wang, D.; Vanmaekelbergh, D.; Mohwald, H. *Phys. Chem. Chem. Phys.* **2006**, *8*, 3828.
25. Nikolaides, M. G.; Bausch, A. R.; Hsu, M. F.; Dinsmore, A. D.; Brenner, M. P.; Gay, C.; Weitz, D. A. *Nature* **2002**, *420*, 299.
26. Wang, M.-H.; Hu, J.-W.; Li, Y.-J.; Yeung, E. S. *Nanotechnology* **2010**, *21*, 145608.
27. Sellers, H.; Ulman, A.; Shnidman, Y.; Eilers, J. E. *J. Am. Chem. Soc.* **1993**, *115*, 9389.
28. Park, S.; Wasileski, S. A.; Weaver, M. J. *J. Phys. Chem. B* **2001**, *105*, 9719.
29. Lopez, N.; Janssens, T. V. W.; Clausen, B. S.; Xu, Y.; Mavrikakis, M.; Bligaard, T.; Norskov, J. K. *J. Catal.* **2004**, *223*, 232.
30. Wang, Z. L. *J. Phys. Chem. B* **2000**, *104*, 1153.
31. Bae, Y.; Kim, N. H.; Kim, M.; Lee, K. Y.; Han, S. W. *J. Am. Chem. Soc.* **2008**, *130*, 5432.
32. Binder, W. H. *Angew. Chem. Int. Ed.* **2005**, *44*, 5172.
33. Hohreiter, V.; Wereley, S. T.; Olsen, M. G.; Chung, J. N. *Meas. Sci. Technol.* **2002**, *13*, 1072.
34. Park, J. S.; Choi, C. K.; Kihm, K. D. *Meas. Sci. Technol.* **2005**, *16*, 1418.
35. Kendall, K.; Dhir, A.; Du, S. *Nanotechnology* **2009**, *20*, 275701.

36. Joo, T. H., Kim, M. S., Kim, K. *J. Raman Spectrosc.* **1987**, *18*, 57.
37. Taylor, C. E.; Pemberton, J. E.; Goodman, G. G.; Schoenfisch, M. H. *Appl. Spectrosc.* **1999**, *53*, 1212.
38. Jung, H. Y.; Park, Y.-K.; Park, S.; Kim, S. K. *Anal. Chim. Acta* **2007**, *602*, 236.
39. Jiang, J.; Bosnick, K.; Maillard, M.; Brus, L. *J. Phys. Chem. B* **2003**, *107*, 9964.
40. Suzuki, M.; Niidome, Y.; Kuwahara, Y.; Terasaki, N.; Inoue, K.; Yamada, S. *J. Phys. Chem. B* **2004**, *108*, 11660.
41. Moskovits, M. *J. Raman Spectrosc.* **2005**, *36*, 485.
42. Wang, H.; Levin, C. S.; Halas, N. J. *J. Am. Chem. Soc.* **2005**, *127*, 14992.
43. Le Ru, E. C.; Etchegoin, P. G.; Meyer, M. *J. Chem. Phys.* **2006**, *125*, 204701.
44. Oh, M. K.; Yun, S.; Kim, S. K.; Park, S. *Anal. Chim. Acta* **2009**, *649*, 111.